CCG-1423: a small-molecule inhibitor of RhoA transcriptional signaling

Chris R. Evelyn,[1] Susan M. Wade,[1] Qin Wang,[1] Mei Wu,[2] Jorge A. Iñiguez-Lluhí,[1] Sofia D. Merajver,[2,3] and Richard R. Neubig[1,2,3]

Departments of [1]Pharmacology and [2]Internal Medicine and [3]University of Michigan Comprehensive Cancer Center, University of Michigan Medical Center, Ann Arbor, Michigan

Abstract

Lysophosphatidic acid receptors stimulate a $G\alpha_{12/13}$/RhoA-dependent gene transcription program involving the serum response factor (SRF) and its coactivator and oncogene, megakaryoblastic leukemia 1 (MKL1). Inhibitors of this pathway could serve as useful biological probes and potential cancer therapeutic agents. Through a transcription-based high-throughput serum response element-luciferase screening assay, we identified two small-molecule inhibitors of this pathway. Mechanistic studies on the more potent CCG-1423 show that it acts downstream of Rho because it blocks SRE.L-driven transcription stimulated by $G\alpha_{12}$Q231L, $G\alpha_{13}$Q226L, RhoA-G14V, and RhoC-G14V. The ability of CCG-1423 to block transcription activated by MKL1, but not that induced by SRF-VP16 or GAL4-VP16, suggests a mechanism targeting MKL/SRF-dependent transcriptional activation that does not involve alterations in DNA binding. Consistent with its role as a Rho/SRF pathway inhibitor, CCG-1423 displays activity in several *in vitro* cancer cell functional assays. CCG-1423 potently (<1 μmol/L) inhibits lysophosphatidic acid–induced DNA synthesis in PC-3 prostate cancer cells, and whereas it inhibits the growth of RhoC-overexpressing melanoma lines (A375M2 and SK-Mel-147) at nanomolar concentrations, it is less active on related lines (A375 and SK-Mel-28) that express lower levels of Rho. Similarly, CCG-1423 selectively stimulates apoptosis of the metastasis-prone, RhoC-overexpressing melanoma cell line (A375M2) compared with the parental cell line (A375). CCG-1423 inhibited Rho-dependent invasion by PC-3 prostate cancer cells, whereas it did not affect the $G\alpha_i$-dependent invasion by the SKOV-3 ovarian cancer cell line. Thus, based on its profile, CCG-1423 is a promising lead compound for the development of novel pharmacologic tools to disrupt transcriptional responses of the Rho pathway in cancer. [Mol Cancer Ther 2007;6(8):2249–60]

Introduction

Cancer metastasis is a significant medical problem responsible for thousands of deaths every year (1). Metastases arise when dysregulation of one or more cellular processes allows malignant cells to escape the confines of the tissue of origin and establish themselves in alternate sites. These processes include cell adhesion, migration, invasion, extravasation, survival, and proliferation (1). Multiple members of the Rho family of small GTPases play important roles in these cellular processes and in some human tumors (e.g., colon, esophageal, lung, pancreatic, and inflammatory breast cancers), up-regulation of RhoA or RhoC is associated with a poor clinical outcome (2, 3).

Rho GTPases are best known for their effects on the actin cytoskeleton. The three main Rho GTPase subfamilies, RhoA, Rac, and Cdc42, control stress fiber formation, lamellipodia, and filopodia (4), respectively, which are structures important for cell motility. Rac and Cdc42 have been implicated in tumor growth, migration, and invasion in both mouse skin and human breast tumors (5–8). Within the RhoA family (RhoA, RhoB, RhoC, etc.), there is evidence for involvement of both RhoA and RhoC in cancer, with the latter being clearly implicated in multiple malignancies. RhoC is essential for inflammatory breast cancer cell growth, invasion, and survival (9, 10) and more recently was found to be critical for invasion by PC-3 prostate cancer cells (11). Similarly, RhoC is critical for *in vivo* metastasis of polyoma T antigen–induced mammary tumors (12). Clearly, the RhoA family GTPases play important roles in multiple cellular processes central to tumor growth and metastasis.

Heterotrimeric G protein–coupled receptors (GPCR), especially those activating the G12/13 family of Gα subunits, are upstream regulators of the Rho pathway and are also implicated in metastasis. Lysophosphatidic acid (LPA), thrombin, and bombesin, acting on their respective GPCRs, stimulate Rho signaling and migration of various cancer cell lines (13–15). A family of three rhoGEFs containing a regulator of G protein signaling homology (RH) domain serves to couple receptors and $G\alpha_{12/13}$ subunits to RhoA (16). The three RH domain-containing rhoGEFs are p115rhoGEF, PDZ-rhoGEF, and leukemia-associated rhoGEF (LARG). The latter was initially found as a fusion to

Received 12/18/06; revised 5/15/07; accepted 6/29/07.

Grant support: NIH grants R01GM39561 (R.R. Neubig), R01CA77612 (S.D. Merajver), and RO1DK61615 (J.A. Iñiguez-Lluhí); Burroughs Wellcome Fund (S.D. Merajver); Department of Defense (S.D. Merajver); Breast Cancer Research Foundation (S.D. Merajver); and University of Michigan Office of Research and Graduate Studies Translational Grant (R.R. Neubig and S.D. Merajver).

The costs of publication of this article were defrayed in part by the payment of page charges. This article must therefore be hereby marked *advertisement* in accordance with 18 U.S.C. Section 1734 solely to indicate this fact.

Requests for reprints: Richard R. Neubig, Department of Pharmacology, University of Michigan Medical Center, 1301 MSRB III, Room 2220D, 1150 West Medical Center Drive, Ann Arbor, MI 48109-0632. Phone: 734-763-3650; Fax: 734-763-4450. E-mail: RNeubig@umich.edu

doi:10.1158/1535-7163.MCT-06-0782

mixed lineage leukemia in a patient with acute myelogenous leukemia (17). Binding of activated Gα subunits (i.e., $G\alpha_{12}$ and $G\alpha_{13}$) to the RH domain of the rhoGEF stimulates the DH-PH domain-mediated guanine nucleotide exchange on the small GTPase RhoA, leading to its activation (18–20). Another G protein–activated rhoGEF, p63-rhoGEF, is activated by $G\alpha_q$ but does not contain an RH domain (21). Furthermore, the downstream Rho effector Rho-associated coiled coil–forming protein kinase (ROCK) is implicated in migration and invasion of cancer cells (22). Thus, $G\alpha_{12/13}$-coupled receptors can stimulate activation of RhoA as well as downstream cellular processes involved in cancer metastasis.

In addition to its established effects on motility, RhoA-dependent actin polymerization in response to activation of $G\alpha_{12/13}$-coupled GPCRs leads to changes in gene expression. The loss of free G-actin resulting from actin polymerization leads to its dissociation from the transcriptional coactivator megakaryoblastic leukemia 1 (MKL1), which then translocates into the nucleus where it collaborates with serum response factor (SRF) to induce gene expression (23, 24). SRF participates in many cellular processes, including cell growth and differentiation, apoptosis, and angiogenesis (25, 26). Although the role of gene transcription in Rho-related cancer biology is poorly understood, both RhoA and RhoC regulate genes important for cell growth and proliferation, such as *c-fos* and *cyclin D1* (25, 27). RhoC overexpression has been linked to vascular endothelial growth factor-C, CXCL1 chemokine, and fibronectin up-regulation, which are important for angiogenesis and formation of the extracellular matrix (27). In addition, several serum-stimulated genes shown to be MKL1 dependent have been implicated in cancer, including *SRF, adrenomedullin, epiregulin, interleukin-6, hexokinase 2*, and *zyxin* (28). These MKL1-dependent genes participate in various cancer-linked processes, including cell growth, migration, invasion, and survival (25, 26, 29–33). Thus, alterations in gene expression are likely to be an integral part of Rho effects on cancer metastasis.

Currently, there are relatively few drugs or pharmacologic tools that target Rho GTPase family signaling pathways. Much of the effort to date has focused on inhibiting the COOH-terminal isoprenylation of the Rho GTPases. This lipid modification is necessary for membrane localization and function of the activated Rho proteins. The most widely used inhibitors of this modification include farnesyltransferase and geranylgeranyltransferase inhibitors and the cholesterol-lowering statin drugs (34). However, these compounds are not specific for the Rho family of small GTPases so their effects are difficult to interpret mechanistically. There have also been significant efforts aimed at inhibiting the Rho effector molecule ROCK. The ROCK inhibitors Y-27632 and Wf-536 have shown promising antimetastatic activity both *in vitro* and *in vivo* (35–37). To date, the only specific and direct inhibitor of Rho GTPases is the Rac1 inhibitor NSC23766 (38). Although it is relatively specific, it is not very potent (IC_{50}, ~50 μmol/L). Thus, there is a clear need and opportunity for specific inhibitors of Rho GTPase signaling pathways.

In this study, we took advantage of a modified serum response element (SRE)-luciferase reporter to undertake a high-throughput screen aiming to identify novel small-molecule inhibitors of the RhoA family signaling pathway. We chose to use a firefly luciferase expression vector driven by a mutant SRE (SRE.L) lacking the ternary complex factor binding sites because this construct is a selective probe of RhoA-induced gene transcription (39). We initiated Rho pathway signaling through the upstream signals $G\alpha_{13}$ and LARG so that inhibition at any step from $G\alpha_{13}$ to the SRE could be detected. By this approach, we identified two novel and structurally similar small-molecule inhibitors of RhoA-stimulated transcription. Mechanistic analysis showed that the more potent compound (CCG-1423) elicits its effects downstream of RhoA and actin polymerization by a mechanism targeting MKL/SRF-dependent transcriptional activation. Interestingly, we find that CCG-1423 inhibits LPA receptor-stimulated DNA synthesis, cell growth, cell survival, and Matrigel invasion for several cancer cell lines.

Materials and Methods

Plasmids and Reagents

The Rho-responsive SRE.L luciferase reporter construct and myc-tagged human LARG expression plasmid are described in ref. 39. The $p(GAL4)_2$-Luc luciferase reporter was generated by ligation of a 50-bp double-stranded oligonucleotide bearing two idealized GAL4 sites into the *Bam*HI and *Bgl*II sites of pΔODLO2 (40). Control expression vectors driving *Renilla* luciferase, pRL-cytomegalovirus and pRL-thymidine kinase (TK), were from Promega. Human $G\alpha_{12}$Q231L, $G\alpha_{13}$Q226L, RhoA-G14V, and RhoC-G14V expression plasmids were from the UMR cDNA Resource Center. Expression plasmids for MKL1 (41), SRF-VP16 (42), GAL4-MKL1 (amino acids 601–931; ref. 23), and C3 exotoxin (43) were kindly provided by Dr. Michael Parmacek (University of Pennsylvania, Philadelphia, PA), Dr. Li Li (Wayne State University, Detroit, MI), Dr. Ron Prywes (Columbia University, New York, NY), and Dr. John Williams (University of Michigan, Ann Arbor, MI), respectively. The cytomegalovirus-driven NH_2-terminally HA-tagged GAL4-VP16 expression vector was generated by subcloning the coding sequence from a Rous sarcoma virus–driven version (44) into pcDNA3.1. The pcDNA3.1-zeo expression plasmid and mouse laminin were from Invitrogen. The marine toxin latrunculin B as well as daunorubicin, LPA, Igepal, antimouse IgG peroxidase conjugate, and antirabbit IgG peroxidase conjugate were from Sigma. Pertussis toxin (PTX) was from List Biological Laboratories, Inc. BD BioCoat Matrigel invasion chambers (8 μm) were from Becton Dickinson. 5-Bromo-2′-deoxyuridine (BrdUrd), anti-BrdUrd-peroxidase, BM blue peroxidase substrate, and cell proliferation reagent WST-1 were from Roche Diagnostics. The caspase-3 fluorescent

peptide substrate, rhodamine 110, bis-*N*-CBZ-L-aspartyl-L-glutamyl-L-valyl-L-aspartic acid amide was from Biotium. The chemical compounds CCG-977 [N1-(4-([3,5-di(trifluoromethyl)anilino]sulfonyl)-phenyl)-4-chlorobenzamide] and CCG-1423 [*N*-[2-(4-chloroanilino)-1-methyl-2-oxoethoxy]-3,5-bis(trifluoromethyl)benzamide] were from Maybridge. The HEK293T, PC-3, SKOV-3, and A375M2 cell lines were kind gifts from Drs. J. Menon, Kenneth Pienta, and Kathleen Cho (University of Michigan) and Dr. Richard Hynes (Massachusetts Institute of Technology, Cambridge, MA). The A375, WI-38, and SW962 cell lines were obtained from the American Type Culture Collection. The SK-Mel-28 and SK-Mel-147 cell lines have been described previously (45, 46).

Cell Culture, Transfections, and Dual-Luciferase Assay

Cell lines were normally maintained in DMEM containing 10% fetal bovine serum (FBS), 100 units/mL penicillin, and 100 μg/mL streptomycin at 37°C in 5% CO_2. HEK293T or PC-3 cells were seeded into 96-well plates (3×10^4 to 4×10^4 per well) 24 h before transfection. Cells were transiently transfected by incubation with the indicated amounts of DNA plasmids plus 1 μL of LipofectAMINE 2000 (Invitrogen) per μg of DNA in antibiotic-free culture medium. For dual-luciferase measurements, various activator plasmids (i.e., $G\alpha_{12}$Q231L, $G\alpha_{13}$Q226L, RhoA-G14V, RhoC-G14V, MKL1, SRF-VP16, GAL4-VP16, and GAL4-MKL1) were included along with the SRE.L or p(GAL4)$_2$-Luc luciferase reporter and PRL-TK or PRL-cytomegalovirus *Renilla* control plasmids. The total amount of DNA was kept constant by inclusion of the appropriate amount of pcDNA3.1. Transfection efficiencies determined with pcDNA3.1-eGFP were approximately 90% to 100% and 30% to 50% for HEK293T and PC-3 cells, respectively. Five to 6 h after transfection, the transfection mixture was removed and cells were starved overnight in DMEM containing 0.5% FBS and 1% penicillin-streptomycin. Firefly and *Renilla* luciferase activities were determined 18 to 19 h later using the dual-luciferase assay kit (Promega) according to the manufacturer's instructions. Luminescence was read on a Victor plate reader with dual injectors (Perkin-Elmer). (The effects of CCG-1423 on serum- and LPA-induced stress fibers were minimal. There were some LPA-stimulated cells showing a change in the morphology of phalloidin staining with 5 μmol/L CCG-1423, but most samples showed nearly normal stress fiber formation.) In the site of action studies, firefly luciferase activity was normalized to *Renilla* luciferase activity. For testing chemical compounds, 1 μL of compound or DMSO was added to the cells (final concentration, 1% DMSO) at the beginning of the serum starvation step.

High-Throughput SRE.L Luciferase Screen

HEK293T cells (6×10^6 per dish) were seeded into 10-cm dishes 24 h before transfection. Cells were cotransfected with 5 ng of $G\alpha_{13}$Q226L, 150 ng of LARG expression plasmids, and 3 μg of the SRE.L reporter plasmid. Two thousand chemical compounds (Maybridge) were prespotted onto white 96-well Costar tissue culture plates (Corning) in 1 μL DMSO (final concentration of compounds, 10 μmol/L) using a Biomek FX Workstation (Beckman Coulter). Cells were trypsinized 5 to 6 h after transfection and transferred to the compound-containing assay plates (3×10^4 per well) in 100 μL DMEM containing 0.5% FBS and 1% penicillin-streptomycin. After an additional 18 to 19 h of incubation, the robotic workstation was used to remove 70 μL of medium from each well and to add 30 μL of Steady-Glo reagent (Promega). Plates were incubated for 30 min at room temperature with rocking and luminescence was read for 1 s/well on the Victor plate reader. The statistical Z′ factor (47) for high-throughput assays was calculated by using the following formula: $Z' = 1 - [(3\sigma_{c+} + 3\sigma_{c-}) / (|\mu_{c+} - \mu_{c-}|)]$ (σ = SD, μ = mean, c+ = latrunculin B, and c− = DMSO-negative control).

Stress Fiber Formation

NIH3T3 mouse fibroblast cells (5.0×10^5 per well) were plated onto coverslips in six-well plates. After attachment, cells were serum starved overnight in serum-free DMEM (0% calf serum). Cells were pretreated with compounds for 1 h before the addition of LPA (30 μmol/L) or calf serum (10%). On addition of the stimuli, the cells were incubated for an additional 1 h. Wells were then washed with PBS and fixed for 15 min with 4% paraformaldehyde. Cells were then washed again with PBS and then lysed in buffer containing 0.3% Triton X-100 in PBS for 15 min. After washing in buffer containing 0.5% Igepal in PBS, cells were incubated for 1 h with rhodamine-phalloidin (1:200) stain in PBS containing 0.5% Igepal and 1% bovine serum albumin. Cells were then washed twice in 0.5% Igepal in PBS and then mounted onto slides with Gel Mount antifade solution (Biomeda). Cell images were obtained with an Olympus FluoView 500 microscope with a 60× oil objective.

DNA Synthesis

PC-3 human prostate cancer cells (1.2×10^4 per well) were plated onto 96-well plates coated with laminin. After attachment, cells were serum starved overnight in serum-free (0% FBS) DMEM and treated with LPA (100 μmol/L) or FBS (10%) for 27 h. BrdUrd (10 μmol/L final) was added to the wells during the final 4.5 h of the incubation. Wells were then washed with PBS and fixed for 20 min with 100 μL of 70% ethanol in 2.3 mol/L HCl. After washing with 10% FCS in PBS, cells were incubated for 1 h at room temperature with anti-BrdUrd-peroxidase. Wells were washed with PBS and then BM blue peroxidase substrate was added, and after 30 min, the reaction was stopped by the addition of 2 N H_2SO_4. The absorbance was read at 450 nm using a Victor plate reader. To determine cell viability, the tetrazolium salt WST-1 was added to the wells during the last 1 h of incubation with BrdUrd. The mitochondrial metabolite of WST-1 cleavage was detected spectrophotometrically at 450 nm just before washing and fixing the cells for BrdUrd measurements.

Cell Growth

Cells in normal culture medium were plated (2,000 per well) in a 96-well plate coated with laminin. After attachment, the medium was replaced with serum-free medium (0% FBS) with 30 μmol/L LPA with or without

300 nmol/L CCG-1423. Fresh LPA with or without CCG-1423 was added at day 5 to ensure that LPA and compound were present throughout the experiment. On day 8, WST-1 reagent was added to the wells for 1 h and absorbance at 450 nm was read using a Victor plate reader.

Caspase-3 Activity

Cells in normal culture medium were plated (2×10^4 per well) in a black 96-well plate coated with laminin. After overnight attachment, the medium in the wells was replaced with serum-free DMEM (0% FBS) with CCG-1423 or daunorubicin for 25 h. An equal volume of 2× reaction buffer [20 mmol/L PIPES (pH 7.4), 2 mmol/L EDTA, 0.2% CHAPS, 10 mmol/L DTT] containing 50 μmol/L of the fluorogenic caspase-3 substrate Z-DEVD-R110 was then added. After an additional 90 min of incubation at 37°C, fluorescence was measured in a Victor plate reader using excitation at 485 nm and emission detection at 520 nm.

Matrigel Cell Invasion

PC-3 or SKOV-3 cells (5×10^4) were transferred to 24-well Matrigel inserts in serum-free medium with or without CCG-1423. Serum-free medium (0% FBS) with or without 30 μmol/L LPA as chemoattractant was added to the lower well, and the invasion chambers were returned to the incubator for 24 h. Inserts were fixed in methanol for 10 min and then stained 30 min with 0.5% crystal violet in 20% methanol. After wiping the top surface of the filter to remove noninvaded cells, the number of remaining cells was determined by counting four nonoverlapping 20× fields. For PTX experiments, cells were treated with 100 ng/mL PTX overnight before being transferred to the Matrigel inserts and 100 ng/mL PTX was maintained in the medium.

Results

Rho-Dependent SRE.L Luciferase Regulation

To assess the suitability of the mutant SRE.L luciferase reporter (which lacks the ternary complex factor–binding sites present in the normal SRE) as a high-throughput assay for inhibitors of GPCR-regulated Rho-dependent pathways (Fig. 1A), we tested a series of Rho pathway activators beginning with $G\alpha_{13}$ and LARG. As shown in Fig. 1B, cotransfection of HEK293T cells with expression vectors for the constitutively active mutant Gα subunit $G\alpha_{13}Q226L$ together with LARG activates the SRE.L-driven reporter synergistically (i.e., 1.6-fold above the sum of the independent stimulation by $G\alpha_{13}Q226L$ and LARG). In Fig. 1C, effective stimulation is also observed for a constitutively active $G\alpha_{12}$ guanine nucleotide-binding protein, $G\alpha_{12}Q231L$, as well as the active Rho GTPases RhoA-G14V and RhoC-G14V. In addition, the SRE.L-driven reporter can be directly stimulated by expression of either the SRF coactivator MKL1 or the chimeric activator SRF-VP16 in which the potent VP16 viral transactivation domain is fused to full-length SRF (Fig. 1C). Thus, the pathway can be activated using signals either upstream ($G\alpha_{13}$ and/or LARG) or downstream (MKL1 or SRF-VP16) of RhoA and RhoC. As shown in the signaling pathway diagram (Fig. 1A), Rho-mediated SRE.L luciferase stimulation is dependent on actin polymerization and the ensuing monomeric G-actin depletion. Therefore, we examined the effect of the marine toxin latrunculin B, which binds to G-actin and inhibits actin polymerization, for its ability to inhibit $G\alpha_{13}Q226L$-stimulated SRE.L-driven luciferase expression. As shown in Fig. 1D, 0.5 μmol/L latrunculin B completely abrogates the $G\alpha_{13}Q226L$ stimulation, confirming that our SRE.L system is indeed dependent on actin polymerization. Lastly, to ensure that the SRE.L reporter response is Rho dependent, we cotransfected cells with expression vectors for both $G\alpha_{13}Q226L$ and the *Clostridium botulinum* exotoxin C3. ADP-ribosylation of Rho by the C3 exotoxin results in Rho inactivation. $G\alpha_{13}Q226L$-stimulated SRE.L luciferase expression is nearly abolished by the C3 exotoxin (Fig. 1D), showing the Rho dependence of the response.

High-Throughput Screen for Rho Pathway Inhibitors

To identify novel chemical inhibitors of the RhoA pathway, we first adapted the SRE.L luciferase assay to a high-throughput format using 293T cells coexpressing $G\alpha_{13}Q226L$ and LARG. Statistical analysis to determine the robustness and reproducibility of the assay for high-throughput screening yielded a Z′ factor of 0.7 (see Materials and Methods), which indicates that it is well suited for our purposes. Using this assay, we screened a 2,000-compound subset of the Maybridge diverse chemical compound collection. The results of the screen are summarized in Fig. 2A. Applying a stringent cutoff of >75% inhibition and using the actin polymerization inhibitor latrunculin B as a positive control, we obtained 39 candidates. We used the dual-luciferase format (see Materials and Methods) as a follow-up assay to confirm the initial results and to test for nonspecific cellular toxicity or general transcriptional inhibition. Of the original 39 hits, we confirmed inhibition of the SRE.L luciferase expression for 18 compounds. Of these, 13 also inhibited cytomegalovirus *Renilla* luciferase expression, suggesting a generalized transcriptional inhibition or nonspecific cellular toxicity. This yielded five confirmed hits, of which four were available for resupply from Maybridge. A common problem in high-throughput, luciferase-based inhibitor screens is the potential for the recovery of direct luciferase enzyme inhibitors. Of the four compounds isolated in the screen, two inhibited firefly luciferase in cell lysates, indicating that they inhibited the reporter enzyme directly rather than its cellular expression. Thus, out of 2,000 compounds screened, we identified 2 lead compounds, CCG-977 and CCG-1423, as specific inhibitors of the RhoA pathway based on our criteria. Strikingly, these compounds share substantial structural similarity because they contain identical R1 (3,5-bis-trifluoromethylphenyl) and R2 (*p*-chlorophenyl) groups connected by distinct linkers. CCG-977 has an aromatic linker with eight atoms separating the two R groups, whereas CCG-1423 has an aliphatic linker with six atoms between R1 and R2 (Fig. 2B).

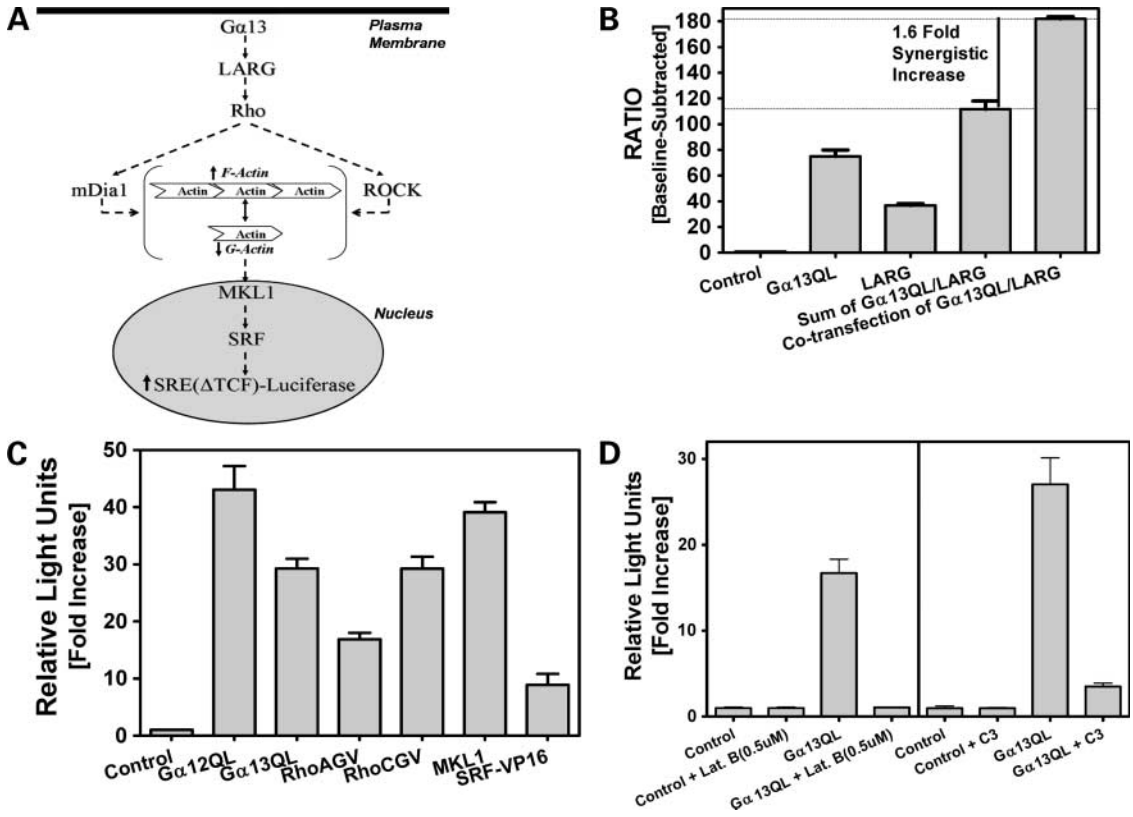

Figure 1. Characterization of the SRE.L system in HEK293T cells. **A,** Gα13 activates the rhoGEF LARG, which activates Rho. This leads to actin polymerization through mDia1 and ROCK. On actin polymerization, the coactivator MKL1 is released from actin and translocates into the nucleus. There, MKL1 interacts with the transcription factor SRF and the complex activates the SRE(ΔTCF) response element, leading to luciferase expression. **B,** $G\alpha_{13}$Q226L and LARG synergistically stimulate SRE.L-mediated transcription. HEK293T cells were cotransfected with 0.5 ng of $G\alpha_{13}$Q226L and/or 0.2 ng of LARG expression plasmids along with 30 ng of SRE.L and 3 ng of PRL-TK reporter plasmids. *Dotted line,* sum of luciferase activities for $G\alpha_{13}$ and LARG expressed individually. Cotransfection produces a 1.6-fold synergistic activation. **C,** constitutively active mutants of several activators stimulate SRE.L. Expression plasmids for constitutive activators (0.1 ng of $G\alpha_{12}$Q231L and $G\alpha_{13}$Q226L, 10 ng of RhoA-G14V and RhoC-G14V, and 1 ng SRF-VP16) or for wild-type MKL1 (3 ng) were individually cotransfected with 15 ng of SRE.L reporter plasmid. **D,** the actin polymerization inhibitor latrunculin B and the Rho inactivator C3 exotoxin inhibit $G\alpha_{13}$Q226L-stimulated SRE.L-driven luciferase expression. Cells were cotransfected with 0.3 ng of the $G\alpha_{13}$Q226L expression plasmid and 15 ng of the SRE.L reporter plasmid with or without 50 ng of the C3 expression plasmid. At the beginning of serum starvation, cells were treated with 0.5 μmol/L latrunculin B or 1% DMSO for 18 to 19 h and harvested as described in Materials and Methods. The pcDNA3.1-zeo plasmid was used as carrier DNA in all experiments, which were done in triplicate. Data from **B** were baseline subtracted and normalized to the *Renilla* internal control and expressed as a ratio of firefly to *Renilla* luciferase activities. Data from **C** and **D** are expressed as fold increase above baseline. Data in **B, C**, and **D** were measured in triplicate and are representative data of $n = 3$. The raw firefly luciferase counts (in thousands) for the *left half of the graph* in **D** were 200 ± 40 and 3,300 ± 600 for control and $G\alpha_{13}$Q226L, respectively. The raw firefly luciferase counts (in thousands) for the *right half of the graph* in **D** were 18 ± 8 and 492 ± 97 for control and $G\alpha_{13}$Q226L, respectively.

CCG-977 and CCG-1423 Inhibit Rho Pathway-Induced Transcription

To further assess whether CCG-977 and CCG-1423 selectively inhibit transcription induced by the Rho pathway, we examined the effect of these compounds on $G\alpha_{13}$Q226L-stimulated firefly luciferase expression driven by the SRE.L response element and *Renilla* expression from the constitutively active TK promoter in PC-3 prostate cancer cells. Both compounds inhibited SRE.L luciferase expression with IC_{50} values of 1 to 5 μmol/L while only modestly inhibiting TK-driven *Renilla* expression (Fig. 3A and B). The extent of inhibition of *Renilla* expression correlated with inhibition of cell viability as detected by WST-1 absorbance (data not shown). Similar to the effect of CCG-977 and CCG-1423, latrunculin B potently inhibited the luciferase signal and also showed a modest effect on the TK *Renilla* signal at the highest concentrations (Fig. 3C). In contrast, the general inhibitor of transcription 5,6-dichlorobenzimidazole-1-β-D-ribofuranoside, which functions as an inhibitor of kinases of the RNA polymerase COOH-terminal domain, inhibited firefly and *Renilla* luciferase expression equally (Fig. 3D). Thus, CCG-1423 and CCG-977 have selective effects on SRF-mediated transcription activated by Rho pathway signaling in comparison with TK promoter-mediated transcription.

CCG-1423 Inhibits Downstream of Rho

To determine the site of action of CCG-1423, we activated the Rho signaling pathway in PC-3 cells at multiple steps. CCG-1423 (10 μmol/L) inhibited SRE.L activation by heterotrimeric G proteins ($G\alpha_{12}$Q231L and $G\alpha_{13}$Q226L; Fig. 4A).

A

Total # of Compounds Screened	**2000**
Hits from Primary Screen (Steady-Glo Luciferase Assay)	**39 (2%)**
Secondary Screen/Dose Response (Dual Flash Luciferase Assay)	21 – Didn't inhibit SRE-Luciferase 13 – Inhibited Renilla **5 – Confirmed hits (0.25%)**
Available for Re-Supply	**4 (0.2%)**
Direct inhibition of Firefly Luciferase	2 – Direct inhibitors of Firefly Luciferase **2 – True Positives (0.1%)**

B

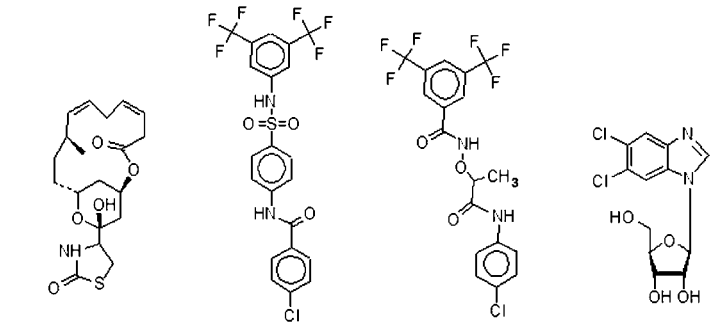

Figure 2. Summary of high-throughput screening results and chemical structures. **A,** two thousand chemical compounds from the Maybridge Diverse Chemical Library collection were screened using the SRE.L assay as described in Materials and Methods. Thirty-nine compounds inhibited the SRE.L response by ≥75%. Five of the 39 compounds selectively inhibited firefly luciferase but not cytomegalovirus *Renilla* luciferase expression. Four compounds were available for resupply from Maybridge and two did not directly inhibit firefly luciferase activity. All studies were done in HEK293T cells. **B,** the actin polymerization inhibitor latrunculin B was our positive control for the screen. Structures of CCG-977 and CCG-1423, the two lead compounds that came out of the screen. The kinase inhibitor 5,6-dichlorobenzimidazole-1-β-D-ribofuranoside (*DRB*) is a general transcription inhibitor.

[Control experiments testing the effect of CCG-1423 on activator protein expression (e.g., LARG, RhoA, and MKL1) could not be interpreted as we were unable to detect the expression of the tagged proteins in PC-3 cells by Western blots with concentrations of plasmids relevant to the luciferase assay.] This result indicates that the inhibitor is not specific for $G\alpha_{13}$ because $G\alpha_{12}$ signals are also affected. Notably, CCG-1423 does not seem to interfere with Rho activation per se (by targeting LARG for example) because acute treatment with CCG-1423 did not inhibit LPA- or serum-stimulated stress fiber formation in NIH3T3 mouse fibroblasts (Fig. 4B). CCG-1423, however, inhibited the activity elicited by expression of RhoA-G14V and RhoC-G14V. Because activation by these proteins is not dependent on upstream activators, this further supports an action of the compound at a downstream step. The ability to block signals initiated by both RhoA and RhoC indicates that the step inhibited by CCG-1423 is engaged by both proteins. This does not seem to be the Rho kinase (ROCK) because CCG-1423 does not inhibit ROCK kinase activity *in vitro* nor does the known ROCK inhibitor Y-27632 fully inhibit $G\alpha_{13}$-stimulated SRE-luciferase expression (Supplementary Fig. S1).[4] Thus, CCG-1423 should be capable of disrupting cancer cell functions elicited by RhoC as well as RhoA.

Because the data above indicate that CCG-1423 does not interfere with upstream components of the pathway, we probed steps more proximal to the transcriptional machinery. To this end, we tested effects of the compound on the transcriptional response induced by several transcription factors/coactivators. SRE.L-driven transcription is dependent on the ability of SRF to bind to this DNA element and nucleate the assembly of productive transcription complexes. CCG-1423 could therefore act by interfering with SRE-SRF recognition or by altering SRF-specific mechanisms of transcriptional activation. To distinguish between these possibilities, we examined the ability of CCG-1423 to inhibit activity elicited by an SRF-VP16 fusion protein. This chimera depends on the SRF-SRE interaction for its recruitment to the promoter but can activate transcription through the VP16 activation domain. As can be seen in Fig. 4A, CCG-1423 failed to inhibit the activity elicited by this protein, suggesting that the compound does not interfere with SRE-SRF interactions and implies that it does not affect transcriptional activation pathways used by the VP16 activation domain. This last point is confirmed by the observation that CCG-1423 does not inhibit the transcriptional response elicited by the chimeric activator GAL4-VP16 at a promoter-bearing GAL4 sites (Fig. 4A).

To examine the effects of CCG-1423 on transcriptional activation mechanisms used by SRF, we tested the ability of this compound to inhibit SRE.L-driven transcription stimulated by expression of the SRF coactivator MKL. As can be seen in Fig. 4A, despite the fact that expression of MKL1 led to a robust activation, reaching levels comparable with those achieved with the SRF-VP16 fusion (31,100 ± 17,500 and 28,500 ± 13,200, respectively), CCG-1423 was able to

[4] Supplementary material for this article is available at Molecular Cancer Therapeutics Online (http://mct.aacrjournals.org/).

inhibit this response effectively, whereas it had no effect on SRF-VP16–mediated activity. Together with the lack of effect on GAL4-VP16 or TK-driven *Renilla* luciferase expression, this result suggests that the compound specifically interferes with SRF/MKL1-dependent transcriptional activation mechanisms. The ability of CCG-1423 to inhibit MKL1-stimulated activity could be due to alterations in the recruitment of MKL to SRF or to effects on MKL1-dependent postrecruitment transcriptional activation mechanisms. As an initial step to explore these possibilities, we bypassed the SRF-dependent MKL recruitment step by fusing a COOH-terminal region of MKL, which harbors a strong activation function to the GAL4 DNA-binding domain. Activity of this fusion protein at a promoter-bearing GAL4 sites was partially inhibited by CCG-1423 (Fig. 4A). The partial nature of the response argues that CCG-1423 may function by altering steps both upstream of MKL recruitment as well as by interfering with postrecruitment functions of MKL at the promoter. Thus, in the context of the current view of the Rho signaling pathway shown in Fig. 1A, our overall analysis indicates that the site of action of CCG-1423 lies at a common step downstream of RhoA and RhoC distinct from the SRF-SRE interaction. Actions on some aspect of MKL1/SRF function (e.g., nuclear translocation, posttranslational modifications, MKL/SRF interaction, or MKL interactions with the transcriptional machinery) seem most likely.

CCG-1423 Inhibits Cancer Cell Functions *In vitro*

The above data show that CCG-1423 exerts selective effects on Rho-stimulated transcription. To determine whether the influence of this compound extends to Rho-mediated cellular responses central to malignant cell growth and metastasis, we have examined the effect of this compound on the growth and invasiveness of cancer cell lines that differ in their Rho pathway properties. Initially, we examined the effects of CCG-1423 on proliferation in response to activation of the Rho pathway. LPA is a major mitogen acting through GPCRs. Specific LPA receptors can activate signaling through at least three different G protein families ($G\alpha_i$, $G\alpha_q$, and $G\alpha_{12}/G\alpha_{13}$). $G\alpha_i$ signaling is sensitive to PTX, whereas $G\alpha_q$ and $G\alpha_{12/13}$ signaling are not. The downstream effects are also distinct because $G\alpha_i$ activates ras (48), $G\alpha_{13}$ strongly activates Rho, whereas $G\alpha_q$ activation leads to both Rho and ras signals (49, 50). Our laboratory has previously shown that LPA stimulates Rho in PC-3 cells through PDZ-rhoGEF (51). We therefore examined the effect of CCG-1423 on LPA-stimulated DNA synthesis in PC-3 cells using a BrdUrd incorporation assay. CCG-1423 specifically inhibited LPA-stimulated DNA synthesis in a dose-dependent manner and completely suppressed this response at 3 μmol/L (Fig. 5A). In this context, PTX had no effect on LPA-stimulated DNA synthesis (data not shown). This is consistent with a model in which LPA activates Rho through non-$G\alpha_i$ pathways, such as $G\alpha_{12}/G\alpha_{13}$ or $G\alpha_q$, which in turn leads to Rho pathway signaling events that are blocked by CCG-1423. Notably, over the 24-h time course of this study, the compound did not affect cell viability as measured by WST-1 metabolism, showing that, at these doses, the compound does not have acute nonspecific toxic effects on PC-3 cells (data not shown).

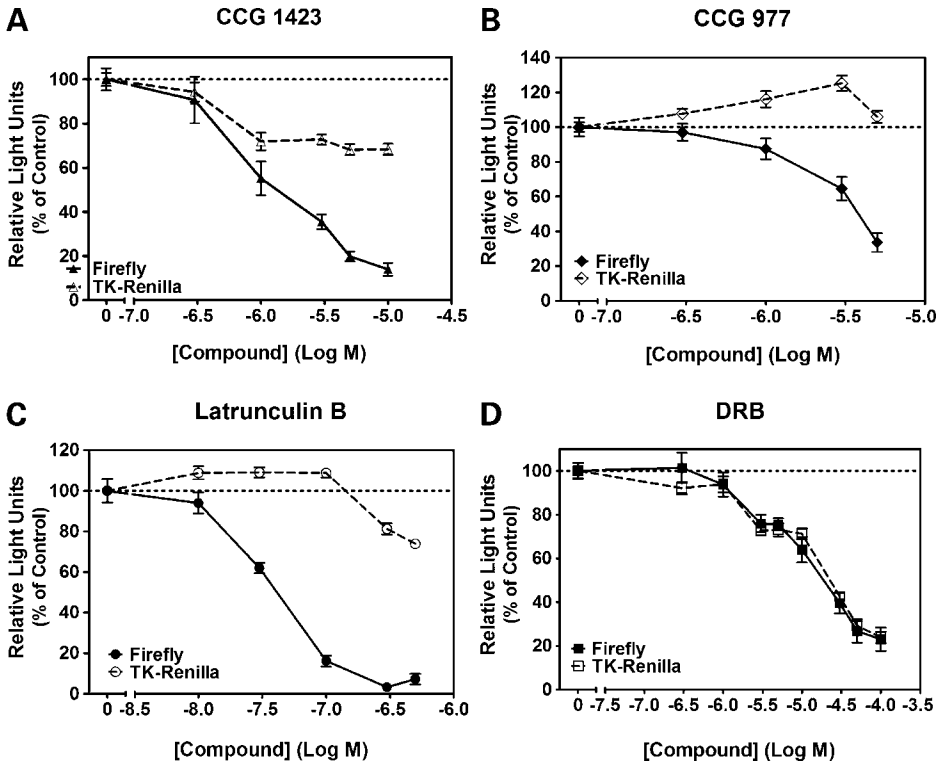

Figure 3. Latrunculin B, CCG-977, and CCG-1423 inhibit $G\alpha_{13}$Q226L-stimulated SRE.L luciferase expression in PC-3 cells. Cells were cotransfected with 1 ng of the $G\alpha_{13}$Q226L expression plasmid along with 30 ng of SRE.L and 7 ng of PRL-TK reporter plasmids as described in Materials and Methods. Cells were treated with the indicated concentrations of compounds, CCG-1423 (**A**), CCG-977 (**B**), latrunculin B (**C**), and 5,6-dichlorobenzimidazole-1-β-D-ribofuranoside (**D**), for 18 to 19 h after transfection before lysis and reading luminescence in the plate reader as described in Materials and Methods. The pcDNA3.1-zeo expression plasmid was used as carrier DNA in all experiments. Data are graphed as a percentage of the DMSO-negative control. *Points,* mean of three separate experiments done in triplicate; *bars,* SE. For the firefly luciferase, data with reporter alone (i.e., without activator) were subtracted.

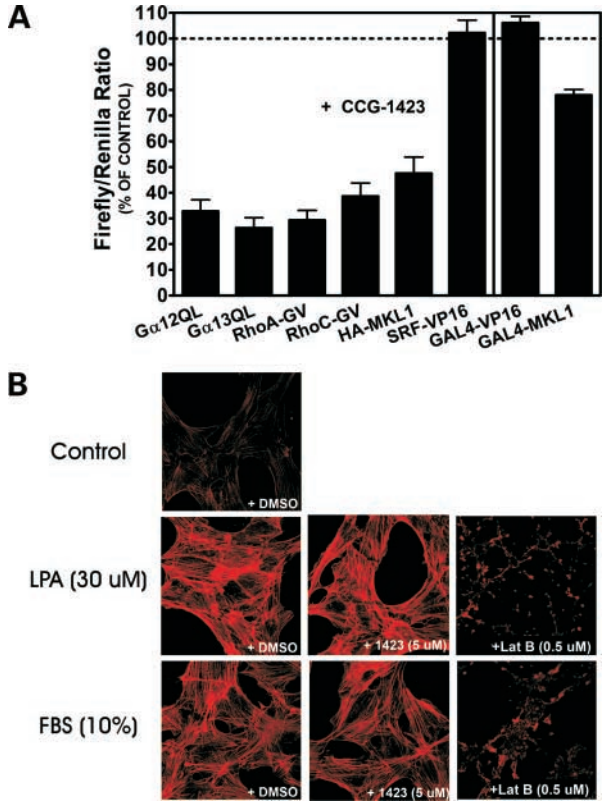

Figure 4. CCG-1423 inhibits downstream of Rho and shows specificity for SRE.L-mediated transcription. **A,** PC-3 cells were individually cotransfected with various activator expression plasmids (1 ng $G\alpha_{12}Q231L$, 1 ng $G\alpha_{13}Q226L$, 3 ng RhoA-G14V, 3 ng RhoC-G14V, 0.2 ng MKL1, 1 ng SRF-VP16, 0.03 ng GAL4-VP16, and 0.01 ng GAL4-MKL1) along with 30 ng of SRE.L or 50 ng of $p(GAL4)_2$-Luc and 7 ng of PRL-TK reporter plasmids. Cells were treated with 10 μmol/L CCG-1423 for 18 to 19 h after transfection during serum starvation. **B,** serum-starved NIH3T3 cells were pretreated with CCG-1423 (5 μmol/L) or latrunculin B (0.5 μmol/L) for 1 h before treatment with LPA (30 μmol/L) and calf serum (10%) for 1 h to stimulate stress fiber formation. Cells were then fixed, lysed, and stained as described in Materials and Methods. Data in **A** are baseline subtracted (reporter alone without activator), and the ratio of firefly to *Renilla* counts is expressed as a percentage of the DMSO control. Experiments were done in triplicate and represent $n = 3$.

To assess the antiproliferative effects of CCG-1423, we analyzed the sensitivity of a panel of cell lines that differ in their Rho pathway properties. The panel includes melanoma lines that overexpress RhoC (A375M2 and SK-Mel-147) as well as related low RhoC-expressing lines (A375 and SK-Mel-28). In addition, we also examined transformed (SW962, PC-3, and SKOV-3) and nontransformed (WI-38) cell lines. The A375M2 line was originally derived from the A375 melanoma line by selection for high metastatic potential by two passages through a mouse lung metastasis system (52). In this line, RhoC mRNA expression is 3- to 5-fold higher than in the nonmetastatic cells remaining in the primary tumor site (52). The SK-Mel-147 line shows substantially higher RhoC protein expression compared with SK-Mel-28 cells as assessed by Western blot (45).

In an 8-day growth assay in the presence of LPA (Fig. 5B), a low concentration of CCG-1423 (300 nmol/L) markedly inhibited the proliferation of RhoC-overexpressing melanoma cells (A375M2 and SK-Mel-147) while not affecting their related low RhoC-expressing counterparts (A375 and SK-Mel-28). The squamous cell cancer line SW962, shown by Sahai and Marshal (22) to exhibit Rho-independent invasion, in contrast to the Rho-dependent A375M2, was similarly unaffected. PC-3 prostate cancer cells, SKOV-3 ovarian carcinoma cells, as well as the nontransformed WI-38 human fibroblasts were inhibited only marginally at this low concentration. However, growth of PC-3 prostate cancer cells was inhibited in this 8-day study with an IC_{50} of 1 μmol/L in good agreement with its potency in effects on DNA synthesis and SRE-mediated gene transcription. The spectrum of activity of CCG-1423 in this panel of cell lines is consistent with its role as a Rho/SRF pathway inhibitor because its antiproliferative effects display selectivity toward RhoC-overexpressing melanoma cell lines. One potential mechanism for reduced growth in the presence of CCG-1423 could be enhanced apoptosis. We therefore measured caspase-3 activation in response to either CCG-1423 or daunorubicin in the RhoC-overexpressing A375M2 and low RhoC-expressing A375 melanoma cell lines. Compared with the low RhoC-expressing A375 line, CCG-1423 induced a 2-fold higher caspase-3 activity in the RhoC-overexpressing (A375M2) derivative (Fig. 5C, *left*). In this cell line, the activity induced by CCG-1423 was nearly as large as the effect of daunorubicin. In contrast to CCG-1423, the effect of daunorubicin (Fig. 5C, *right*) is substantially higher in the low RhoC-expressing A375 cells compared with the RhoC-overexpressing A375M2 cells. These data indicate that CCG-1423 displays selectivity toward Rho-overexpressing lines and the reversal of specificity of the two compounds (CCG-1423 versus daunorubicin) between A375 and A375M2 cells suggests a distinct mechanism of action for CCG-1423 compared with daunorubicin.

A critical process in metastasis is the ability of malignant cells to invade heterologous tissues. Recently, the invasiveness of PC-3 prostate cancer cells was shown to be dependent on RhoC and $G\alpha_{12}$ (11, 53). Thus, we compared the effects of CCG-1423 on matrix invasion by PC-3 prostate cancer cells and SKOV-3 ovarian cancer cells. In a Matrigel invasion assay, PC-3 cells display high invasion rates and do not require an exogenous stimulus for invasion (Fig. 6A, *left*). In contrast, invasion by SKOV-3 cells is greatly stimulated in the presence of LPA (Fig. 6A, *right*). Invasion in these two cell lines relies on different pathways because LPA-stimulated invasion by SKOV-3 cells was completely eliminated by PTX ($G\alpha_i$ pathway dependent), whereas PC-3 cell invasion was not affected (Fig. 6B). Consistent with a Rho pathway inhibitor function, CCG-1423 (3 μmol/L) strongly suppressed the Rho-dependent invasion by PC-3 cells. A similar effect was seen on PC-3 cells in the presence of LPA (data not shown). In contrast, CCG-1423 did not affect the $G\alpha_i$ pathway-dependent invasion by SKOV-3 cells (Fig. 6B).

Discussion

Recent developments in cancer therapeutics have highlighted the importance of molecularly targeted therapies with a current major emphasis on tyrosine kinases (54, 55). However, there is a strong body of evidence supporting efforts to disrupt signaling by oncogenic GTPases, such as ras and Rho family members. These include blockade of critical lipid modifications by farnesyltransferase and geranylgeranyltransferase inhibitors, statins, and bisphosphonates (34). Inhibitors of Rho kinase have also been evaluated in cancer models (35, 37). In this report, we describe a novel small-molecule inhibitor, which disrupts transcriptional signaling by the RhoA GTPase family. The compound described here (CCG-1423) has nanomolar to low micromolar potency as well as selectivity toward Rho-overexpressing and invasive cancer cell lines for inhibition of DNA synthesis, cell growth, and/or invasion.

The role of RhoA family members, particularly RhoA and RhoC, in cancer cell growth and/or metastasis has become quite clear. Multiple studies correlate RhoA or RhoC overexpression and tumor aggressiveness (2, 3). Suppression of RhoC protein expression reduces invasiveness *in vitro* (11). Furthermore, breast tumors induced by the polyoma virus middle T antigen in a RhoC-deficient mouse show normal growth but a dramatic reduction in metastasis (12). The role of GPCR signaling to Rho is also relevant. A recent study found that a nonsynonymous polymorphism in the RH-containing rhoGEF, PDZ-rhoGEF, was associated with reduced lung cancer risk in a case-control study of Mexican-Americans (56). In addition, Yao et al. (11) report that RhoC plays an important role in Rho-dependent prostate cancer cell invasion. This result correlates with our observation that CCG-1423 inhibits PC-3 prostate cancer cell matrix invasion (Fig. 6B).

In the strongly Rho-overexpressing cell lines (A375M2 and SK-Mel-147), we see an effect of nanomolar concentrations of CCG-1423 on cell growth. Rho-mediated regulation of the cell cycle is complex, involving both Rho and ras pathway components, leading to effects on cyclins A and D1 and on the cyclin-dependent kinase inhibitors $p21^{Waf1/Cip1}$ and $p27^{kip1}$ (57–59). Interestingly, the induction of cyclin D1 by the Rho effector ROCK (59) could be due to Rho-mediated gene transcriptional events. Thus, differential dependence on these cell cycle regulators could underlie the functional differences in cell growth and DNA synthesis that we observe with CCG-1423 on the various cancer cell types.

Furthermore, the growth inhibition in the 8-day experiments could also involve enhanced cell death as well as inhibition of cell cycle progression. Consistent with this, caspase-3 activation in the highly metastatic RhoC-overexpressing A375M2 melanoma cell line was enhanced by CCG-1423 whereas a smaller increase was seen with the parental A375 cell line, whereas just the opposite pattern was seen with daunorubicin.

The precise molecular mechanism of action of CCG-1423 is not clear but our findings indicate that CCG-1423 may disrupt Rho signaling through functional inhibition of SRF transcriptional activity. The data suggest that effects on the coactivator MKL1 are likely, although effects on other SRF regulatory cofactors cannot be ruled out. Nuclear MKL1 function depends on Rho-mediated actin polymerization, which leads to dissociation from G-actin and nuclear translocation of MKL1. Free from G-actin, MKL1 can bind the transcription factor SRF and stimulate transcription (23, 24). MKL1 function is also regulated by posttranslational modifications, including covalent modification by members of the small ubiquitin-like modifier family. Consistent with the effects of sumoylation on sequence-specific transcription factors (60), small ubiquitin-like modifier modification of MKL1 attenuates its transcriptional activation potential (61). Thus, CCG-1423 could modify several aspects of MKL1 function, for example (*a*) preventing release from actin or blocking nuclear translocation of MKL1, (*b*) enhancing sumoylation causing transcriptional repression, (*c*) inhibiting the protein-protein

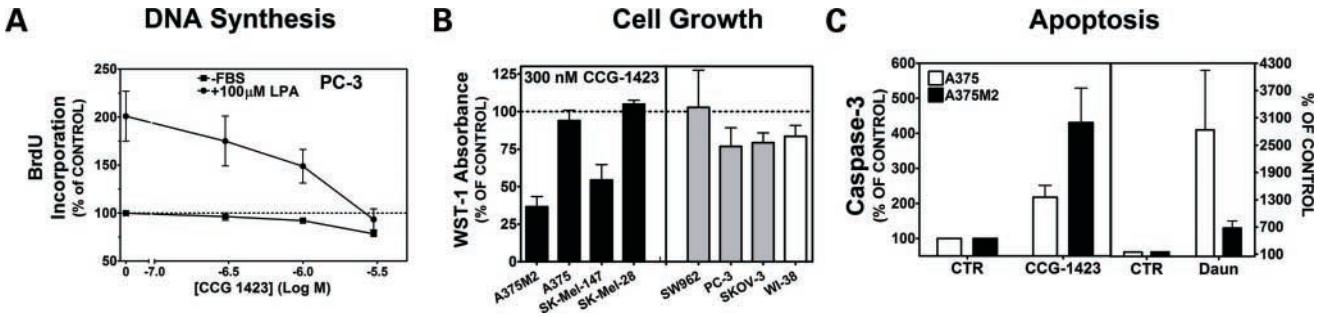

Figure 5. CCG-1423 inhibits cancer cell proliferation and survival. **A,** PC-3 cells were treated for 27 h with 100 μmol/L LPA in the presence or absence of various concentrations of CCG-1423, labeled with BrdUrd, and stained, and absorbance was read as described in Materials and Methods. **B,** various cell lines were treated with 30 μmol/L LPA with or without 0.3 μmol/L CCG-1423, and then on day 8, WST-1 absorbance was read as described in Materials and Methods. *Black columns,* four melanoma lines with differing expression of RhoC [A375M2 and SK-Mel-147 have high expression (see text), whereas the parental line A375 (used to derive A375M2) and SK-Mel-28 have lower expression]; *gray columns,* several other cancer cell lines; *white column,* nontransformed fibroblast line, WI-38. **C,** A375 and A375M2 cells were treated with 3 μmol/L CCG-1423 or 3 μmol/L daunorubicin for 25 h, and then caspase-3 activity was measured with a fluorescent substrate as described in Materials and Methods. In **A** and **C**, data are expressed as a percentage of the no FBS control. In **B**, data are expressed as percentage of the LPA + DMSO control. All data represent $n = 3$.

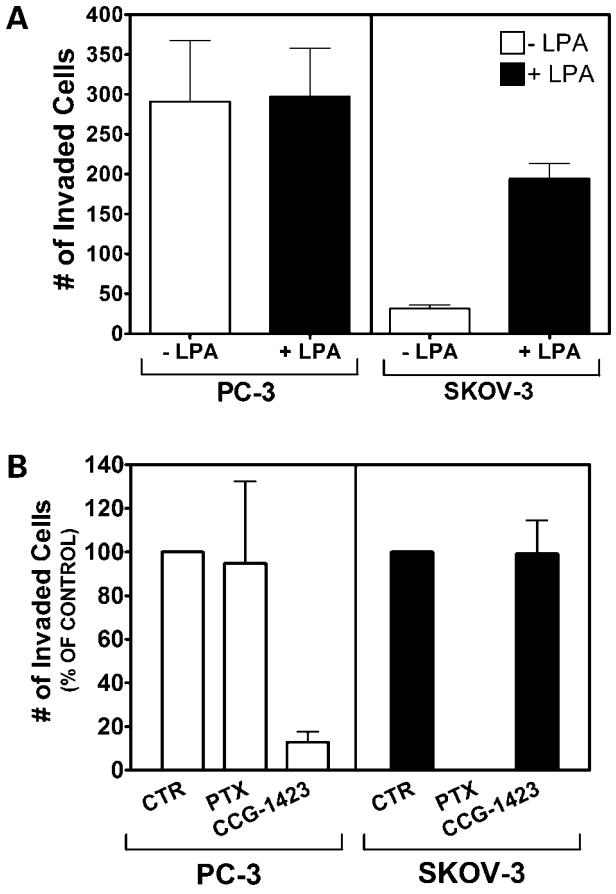

Figure 6. CCG-1423 inhibits prostate cancer cell invasion. **A,** LPA stimulates invasion of SKOV-3 but not PC-3 cells. Invasion of Matrigel-coated filters by serum-starved PC-3 prostate cancer or SKOV-3 ovarian cancer cells was measured with or without 30 μmol/L LPA as chemoattractant as described in Materials and Methods. **B,** CCG-1423 inhibits PC-3 cell invasion, whereas PTX inhibits SKOV-3 cell invasion. The effects of CCG-1423 (3 μmol/L) and PTX (100 ng/mL) on spontaneous (PC-3) or LPA-stimulated (SKOV-3) invasion through Matrigel were measured as described in Materials and Methods. In **B**, data are expressed as a percentage of control. All data represent $n = 3$.

interaction between MKL1 and SRF, or (*d*) disrupting MKL1 coactivator function. The ability of CCG-1423 to partially inhibit the GAL4-MKL1 transcriptional signal supports at least in part this latter point, although definitive conclusions will require additional experiments. Alternatively, CCG-1423 might disrupt some other aspect of SRF function, such as recruitment or activity of other SRF transcription partners (e.g., Nkx3.1 and GATA-4; refs. 62, 63).

The role of different Rho signaling events in cancer biology has been difficult to decipher because RhoA family members activate many effectors, such as Rho kinases (ROCK-I and ROCK-II), rhotekin, and mDia1. The downstream events from Rho signals are similarly diverse, with alterations in actin cytoskeletal organization and gene transcription being two prominent effects. Our identification of CCG-1423 as an inhibitor of Rho-mediated transcription provides a useful tool to further elucidate the role of this process in cancer biology. Given the strong inhibition of PC-3 cell matrix invasion and A375M2 cell growth, it is likely that Rho-stimulated transcriptional processes play a role in these phenomena. Indeed, enhanced Rho-dependent matrix metalloproteinase expression induced by the chemokine CXCL12 acting at CXCR4 receptors is involved in melanoma cell matrix invasion (64). It will clearly be of interest to identify which Rho-dependent genes show reduced expression with CCG-1423.

In summary, our identification of CCG-1423 provides a novel lead compound for the development of more potent and specific inhibitors of Rho-mediated transcription. CCG-1423 should serve both as a pharmacologic tool and as a potential lead for therapeutics for Rho-dependent cancers. Further exploration on the mechanism of action of CCG-1423 and identification of even more potent analogues will be important steps for the future.

Acknowledgments

We thank Dr. Peter Clapp (University of Michigan) for assistance with the actin staining studies; Sergey Chupetra for assistance with the GAL4 transcription studies; Drs. Li Li, Michael Parmacek, and Ron Prywes for kindly providing DNA plasmids; and Drs. J. Menon, Kenneth Pienta, Kathleen Cho, and Richard Hynes for kindly providing cell lines.

References

1. Sawyer TK. Cancer metastasis therapeutic targets and drug discovery: emerging small-molecule protein kinase inhibitors. Expert Opin Investig Drugs 2004;13:1 – 19.

2. Sahai E, Marshall CJ. RHO-GTPases and cancer. Nat Rev Cancer 2002; 2:133 – 42.

3. Faried A, Nakajima M, Sohda M, Miyazaki T, Kato H, Kuwano H. Correlation between RhoA overexpression and tumour progression in esophageal squamous cell carcinoma. Eur J Surg Oncol 2005;31:410 – 4.

4. Whitehead IP, Zohn IE, Der CJ. Rho GTPase-dependent transformation by G protein-coupled receptors. Oncogene 2001;20:1547 – 55.

5. Kwei KA, Finch JS, Ranger-Moore J, Bowden GT. The role of Rac1 in maintaining malignant phenotype of mouse skin tumor cells. Cancer Lett 2006;231:326 – 38.

6. Liang Y, Li C, Guzman VM, et al. Identification of a novel alternative splicing variant of RGS5 mRNA in human ocular tissues. FEBS J 2005; 272:791 – 9.

7. Hirsch DS, Shen Y, Wu WJ. Growth and motility inhibition of breast cancer cells by epidermal growth factor receptor degradation is correlated with inactivation of Cdc42. Cancer Res 2006;66:3523 – 30.

8. Baugher PJ, Krishnamoorthy L, Price JE, Dharmawardhane SF. Rac1 and Rac3 isoform activation is involved in the invasive and metastatic phenotype of human breast cancer cells. Breast Cancer Res 2005;7: R965 – 74.

9. van Golen KL, Davies S, Wu ZF, et al. A novel putative low-affinity insulin-like growth factor-binding protein, LIBC (lost in inflammatory breast cancer), and RhoC GTPase correlate with the inflammatory breast cancer phenotype. Clin Cancer Res 1999;5:2511 – 9.

10. van Golen KL, Wu ZF, Qiao XT, Bao LW, Merajver SD. RhoC GTPase, a novel transforming oncogene for human mammary epithelial cells that partially recapitulates the inflammatory breast cancer phenotype. Cancer Res 2000;60:5832 – 8.

11. Yao H, Dashner EJ, van Golen CM, van Golen KL. Rho C GTPase is required for PC-3 prostate cancer cell invasion but not motility. Oncogene 2006;25:2285 – 96.

12. Hakem A, Sanchez-Sweatman O, You-Ten A, et al. RhoC is dispensable for embryogenesis and tumor initiation but essential for metastasis. Genes Dev 2005;19:1974 – 9.

13. Sawada K, Morishige K, Tahara M, et al. Alendronate inhibits lysophosphatidic acid-induced migration of human ovarian cancer cells by attenuating the activation of rho. Cancer Res 2002;62:6015 – 20.

14. Shi X, Gangadharan B, Brass LF, Ruf W, Mueller BM. Protease-activated receptors (PAR1 and PAR2) contribute to tumor cell motility and metastasis. Mol Cancer Res 2004;2:395 – 402.

15. Lacoste J, Aprikian AG, Chevalier S. Focal adhesion kinase is required for bombesin-induced prostate cancer cell motility. Mol Cell Endocrinol 2005;235:51 – 61.

16. Fukuhara S, Chikumi H, Gutkind JS. RGS-containing RhoGEFs: the missing link between transforming G proteins and Rho? Oncogene 2001; 20:1661 – 8.

17. Kourlas PJ, Strout MP, Becknell B, et al. Identification of a gene at 11q23 encoding a guanine nucleotide exchange factor: evidence for its fusion with MLL in acute myeloid leukemia. Proc Natl Acad Sci U S A 2000;97:2145 – 50.

18. Kozasa T, Jiang X, Hart MJ, et al. p115 RhoGEF, a GTPase activating protein for Gα12 and Gα13. Science 1998;280:2109 – 11.

19. Hart MJ, Jiang X, Kozasa T, et al. Direct stimulation of the guanine nucleotide exchange activity of p115 RhoGEF by Gα13. Science 1998; 280:2112 – 4.

20. Vogt S, Grosse R, Schultz G, Offermanns S. Receptor-dependent RhoA activation in G12/G13-deficient cells: genetic evidence for an involvement of Gq/G11. J Biol Chem 2003;278:28743 – 9.

21. Lutz S, Freichel-Blomquist A, Yang Y, et al. The guanine nucleotide exchange factor p63RhoGEF, a specific link between Gq/11-coupled receptor signaling and RhoA. J Biol Chem 2005;280:11134 – 9.

22. Sahai E, Marshall CJ. Differing modes of tumour cell invasion have distinct requirements for Rho/ROCK signalling and extracellular proteolysis. Nat Cell Biol 2003;5:711 – 9.

23. Cen B, Selvaraj A, Burgess RC, et al. Megakaryoblastic leukemia 1, a potent transcriptional coactivator for serum response factor (SRF), is required for serum induction of SRF target genes. Mol Cell Biol 2003;23: 6597 – 608.

24. Miralles F, Posern G, Zaromytidou AI, Treisman R. Actin dynamics control SRF activity by regulation of its coactivator MAL. Cell 2003;113: 329 – 42.

25. Schwartz DR, Kardia SL, Shedden KA, et al. Gene expression in ovarian cancer reflects both morphology and biological behavior, distinguishing clear cell from other poor-prognosis ovarian carcinomas. Cancer Res 2002;62:4722 – 9.

26. Vickers ER, Kasza A, Kurnaz IA, et al. Ternary complex factor-serum response factor complex-regulated gene activity is required for cellular proliferation and inhibition of apoptotic cell death. Mol Cell Biol 2004;24: 10340 – 51.

27. Wu M, Wu ZF, Kumar-Sinha C, Chinnaiyan A, Merajver SD. RhoC induces differential expression of genes involved in invasion and metastasis in MCF10A breast cells. Breast Cancer Res Treat 2004;84: 3 – 12.

28. Selvaraj A, Prywes R. Expression profiling of serum inducible genes identifies a subset of SRF target genes that are MKL dependent. BMC Mol Biol 2004;5:13.

29. Zudaire E, Martinez A, Cuttitta F. Adrenomedullin and cancer. Regul Pept 2003;112:175 – 83.

30. Andela VB. Correspondence Re: SS Virtanen et al., Alendronate inhibits invasion of PC-3 prostate cancer cells by affecting the mevalonate pathway. Cancer Res 2002;62:2708 – 14. Re K. Sawada et al., Alendronate inhibits lysophosphatidic acid-induced migration of human ovarian cancer cells by attenuating the activation of Rho. Cancer Res 2002;62:6015 – 20. Cancer Res 2004;64:2934 – 5; author reply 2935 – 6.

31. Mathupala SP, Ko YH, Pedersen PL. Hexokinase II: cancer's double-edged sword acting as both facilitator and gatekeeper of malignancy when bound to mitochondria. Oncogene 2006;25:4777 – 86.

32. Yu YP, Luo JH. Myopodin-mediated suppression of prostate cancer cell migration involves interaction with zyxin. Cancer Res 2006;66: 7414 – 9.

33. Zhu Z, Kleeff J, Friess H, et al. Epiregulin is up-regulated in pancreatic cancer and stimulates pancreatic cancer cell growth. Biochem Biophys Res Commun 2000;273:1019 – 24.

34. Fitzgerald K, Tertyshnikova S, Moore L, et al. Chemical genetics reveals an RGS/G-protein role in the action of a compound. PLoS Genet 2006;2:e57.

35. Nakajima M, Katayama K, Tamechika I, et al. WF-536 inhibits metastatic invasion by enhancing the host cell barrier and inhibiting tumour cell motility. Clin Exp Pharmacol Physiol 2003;30:457 – 63.

36. Lawler KM, Foran E, O'Sullivan G, Long A, Kenny D. The mobility and invasiveness of metastatic esophageal cancer is potentiated by shear stress in a ROCK and Ras dependent manner. Am J Physiol Cell Physiol 2006;291:C668 – 77.

37. Nakajima M, Hayashi K, Egi Y, et al. Effect of Wf-536, a novel ROCK inhibitor, against metastasis of B16 melanoma. Cancer Chemother Pharmacol 2003;52:319 – 24.

38. Gao Y, Dickerson JB, Guo F, Zheng J, Zheng Y. Rational design and characterization of a Rac GTPase-specific small molecule inhibitor. Proc Natl Acad Sci U S A 2004;101:7618 – 23.

39. Suzuki N, Nakamura S, Mano H, Kozasa T. Gα12 activates Rho GTPase through tyrosine-phosphorylated leukemia-associated RhoGEF. Proc Natl Acad Sci U S A 2003;100:733 – 8.

40. Subramanian L, Benson MD, Iniguez-Lluhi JA. A synergy control motif within the attenuator domain of CCAAT/enhancer-binding protein α inhibits transcriptional synergy through its PIASy-enhanced modification by SUMO-1 or SUMO-3. J Biol Chem 2003;278:9134 – 41.

41. Du KL, Chen M, Li J, Lepore JJ, Mericko P, Parmacek MS. Megakaryoblastic leukemia factor-1 transduces cytoskeletal signals and induces smooth muscle cell differentiation from undifferentiated embryonic stem cells. J Biol Chem 2004;279:17578 – 86.

42. Hart MJ, Sharma S, elMasry N, et al. Identification of a novel guanine nucleotide exchange factor for the Rho GTPase. J Biol Chem 1996;271: 25452 – 8.

43. Le Page SL, Bi Y, Williams JA. CCK-A receptor activates RhoA through Gα12/13 in NIH3T3 cells. Am J Physiol Cell Physiol 2003;285: C1197 – 206.

44. Chupreta S, Holmstrom S, Subramanian L, Iniguez-Lluhi JA. A small conserved surface in SUMO is the critical structural determinant of its transcriptional inhibitory properties. Mol Cell Biol 2005;25: 4272 – 82.

45. Collisson EA, Kleer C, Wu M, et al. Atorvastatin prevents RhoC isoprenylation, invasion, and metastasis in human melanoma cells. Mol Cancer Ther 2003;2:941 – 8.

46. Soengas MS, Capodieci P, Polsky D, et al. Inactivation of the apoptosis effector Apaf-1 in malignant melanoma. Nature 2001;409: 207 – 11.

47. Zhang JH, Chung TD, Oldenburg KR. A simple statistical parameter for use in evaluation and validation of high throughput screening assays. J Biomol Screen 1999;4:67 – 73.

48. Bian D, Su S, Mahanivong C, et al. Lysophosphatidic acid stimulates ovarian cancer cell migration via a Ras-MEK kinase 1 pathway. Cancer Res 2004;64:4209 – 17.

49. Mills GB, Moolenaar WH. The emerging role of lysophosphatidic acid in cancer. Nat Rev Cancer 2003;3:582 – 91.

50. Chikumi H, Fukuhara S, Gutkind JS. Regulation of G protein-linked guanine nucleotide exchange factors for Rho, PDZ-RhoGEF, LARG by tyrosine phosphorylation: evidence of a role for focal adhesion kinase. J Biol Chem 2002;277:12463 – 73.

51. Wang Q, Liu M, Kozasa T, Rothstein JD, Sternweis PC, Neubig RR. Thrombin and lysophosphatidic acid receptors utilize distinct rhoGEFs in prostate cancer cells. J Biol Chem 2004;279:28831 – 4.

52. Clark EA, Golub TR, Lander ES, Hynes RO. Genomic analysis of metastasis reveals an essential role for RhoC. Nature 2000;406: 532 – 5.

53. Kelly P, Stemmle LN, Madden JF, Fields TA, Daaka Y, Casey PJ. A role for the G12 family of heterotrimeric G proteins in prostate cancer invasion. J Biol Chem 2006;281:26483 – 90.

54. Buchdunger E, Zimmermann J, Mett H, et al. Inhibition of the Abl protein-tyrosine kinase *in vitro* and *in vivo* by a 2-phenylaminopyrimidine derivative. Cancer Res 1996;56:100 – 4.

55. Pollack VA, Savage DM, Baker DA, et al. Inhibition of epidermal growth factor receptor-associated tyrosine phosphorylation in human carcinomas with CP-358,774: dynamics of receptor inhibition *in situ* and antitumor effects in athymic mice. J Pharmacol Exp Ther 1999;291: 739 – 48.

56. Gu J, Wu X, Dong Q, et al. A nonsynonymous single-nucleotide polymorphism in the PDZ-Rho guanine nucleotide exchange factor ($Ser^{1416}Gly$) modulates the risk of lung cancer in Mexican Americans. Cancer 2006;106:2716 – 24.

57. Coleman DE, Sprang SR. Structure of Giα1.GppNHp, autoinhibition in a gα protein-substrate complex. J Biol Chem 1999;274:16669 – 72.

58. Olson MF, Paterson HF, Marshall CJ. Signals from Ras and Rho GTPases interact to regulate expression of p21Waf1/Cip1. Nature 1998; 394:295 – 9.

59. Croft DR, Olson MF. The Rho GTPase effector ROCK regulates cyclin A, cyclin D1, and p27Kip1 levels by distinct mechanisms. Mol Cell Biol 2006;26:4612 – 27.

60. Holmstrom S, Van Antwerp ME, Iniguez-Lluhi JA. Direct and distinguishable inhibitory roles for SUMO isoforms in the control of transcriptional synergy. Proc Natl Acad Sci U S A 2003;100:15758 – 63.

61. Nakagawa K, Kuzumaki N. Transcriptional activity of megakaryoblastic leukemia 1 (MKL1) is repressed by SUMO modification. Genes Cells 2005;10:835 – 50.

62. Belaguli NS, Sepulveda JL, Nigam V, Charron F, Nemer M, Schwartz RJ. Cardiac tissue enriched factors serum response factor and GATA-4 are mutual coregulators. Mol Cell Biol 2000;20:7550 – 8.

63. Jimenez-Sainz MC, Murga C, Kavelaars A, et al. G protein-coupled receptor kinase 2 negatively regulates chemokine signaling at a level downstream from G protein subunits. Mol Biol Cell 2006;17:25 – 31.

64. Bartolome RA, Galvez BG, Longo N, et al. Stromal cell-derived factor-1α promotes melanoma cell invasion across basement membranes involving stimulation of membrane-type 1 matrix metalloproteinase and Rho GTPase activities. Cancer Res 2004;64:2534 – 43.

Molecular Cancer Therapeutics

CCG-1423: a small-molecule inhibitor of RhoA transcriptional signaling

Chris R. Evelyn, Susan M. Wade, Qin Wang, et al.

Mol Cancer Ther 2007;6:2249-2260.